Eur. Phys. J. D (2005)
DOI: 10.1140/epjd/e2005-00215-5

THE EUROPEAN PHYSICAL JOURNAL D

Hyperfine structure and isotope shift study in singly ionized lead

T.J. Wąsowicz, R. Drozdowski, and J. Kwela[a]

Institute of Experimental Physics, University of Gdansk, ul. Wita Stwosza 57, 80-952 Gdansk, Poland

Received 19 April 2005 / Received in final form 9 June 2005
Published online 9 August 2005 –

Abstract. Hyperfine structure and isotope shifts in five optical transitions: 424.5 nm ($6s^2 5f\ ^2\mathrm{F}_{7/2}$–$6s^2 6d^2\ \mathrm{D}_{5/2}$), 537.2 nm ($6s^2 5f\ ^2\mathrm{F}_{7/2}$–$6s6p^2\ ^4\mathrm{P}_{5/2}$), 554.5 nm ($6s^2 7d\ ^2\mathrm{D}_{5/2}$–$6s^2 7p\ ^2\mathrm{P}_{3/2}$), 560.9 nm ($6s^2 7p^2\ \mathrm{P}_{3/2}$–$6s^2 7s\ ^2\mathrm{S}_{1/2}$) and 666.0 nm ($6s^2 7p\ ^2\mathrm{P}_{1/2}$–$6s^2 7s\ ^2\mathrm{S}_{1/2}$) of Pb II have been measured. As a light source the discharge tube was used. The hyperfine structure measurements were performed using metallic isotope ^{207}Pb. For isotope shifts measurements natural lead was used. The high resolution spectral apparatus consisted of a silver coated Fabry-Perot etalon and a grating spectrograph combined with a CCD camera used as a detector. In the analysis of the spectra a computer simulation technique was used. The hyperfine structure observations yielded the splitting constants A for seven levels of Pb II. The isotope shift studies enabled to separate the mass and the field shifts and to determine values of changes of the mean square nuclear charge radii.

PACS. 31.30.Gs Hyperfine interactions and isotope effects, Jahn-Teller effect – 32.10.Fn Fine and hyperfine structure – 32.70.Jz Line shapes, widths, and shifts – 32.30.Jc Visible and ultraviolet spectra – 21.10.Ft Charge distribution

1 Introduction

Isotope shift study is a useful technique of nuclear structure investigations. The total isotope shift (IS) of atomic spectral lines consists of two contributions, this caused by the finite nuclear mass and that resulting from the field effect connected with changes of the mean square nuclear charge radii. The mass effect, which consists of two parts, normal and specific, dominates in very light elements and decreases with increasing Z number. In heavy elements (such as lead) the mass effect is negligible and the field effect, which increases with increasing Z, roughly accounts for the observed shifts.

Lead is the heaviest element with more than one stable isotope. Its stability is a result of the fact that it has a magic number of protons and that the 208 isotope, has a magic number of neutrons, too. The natural lead consists of four stable isotopes of masses 204, 206, 207 and 208. Spectral lines for even isotopes, each with nuclear spin $I = 0$, are always single, but lines of ^{207}Pb, with spin $I = 1/2$, may have as many as four components depending on the J number and splitting of the initial and final energy levels.

If the components of the hyperfine structure (hfs) and IS are resolved their relative intensities and individual positions can easily be determined. Problems arise when the structure is partly or completely unresolved. For such a case the computer simulation technique becomes useful thus getting more information than would be possible by conventional methods. Recently such a computer technique used by us in the analysis of hyperfine structure of lines of Pb I has proved to be efficient and reliable [1,2].

In the present experiment this technique is used to analyse the spectra of five lines of singly ionized lead: 424.5 nm, 537.2 nm, 554.5 nm, 560.9 nm and 666.0 nm. The experiment with ^{207}Pb yields the hfs constants A for levels: $6s^2 7d\ ^2\mathrm{D}_{5/2}$, $6s^2 5f\ ^2\mathrm{F}_{7/2}$, $6s^2 7p\ ^2\mathrm{P}_{3/2}$, $^2\mathrm{P}_{1/2}$, $6s^2 6d\ ^2\mathrm{D}_{5/2}$, $6s^2 7s\ ^2\mathrm{S}_{1/2}$ and $6s6p^2\ ^4\mathrm{P}_{5/2}$. In the experiment with natural lead we have measured the isotope shifts between four stable isotopes. The study has allowed us to separate the two contributions to the total isotope shift, namely the mass and the field shifts, and estimate the changes of the mean square nuclear charge radii. Such a determination for these lines is presented for the first time.

2 Experiment

The experimental arrangement was similar to that used by us before in the hyperfine structure analysis of lines of Pb I [1,2], Sb II [3] and Bi II [4]. In the present work the light source was a quartz discharge tube connected to a vacuum system. To obtain a clear spectrum a very careful outgassing of the tube is necessary. This was accomplished by pumping and heating (to about 900 °C) the tube for a period of several hours. The metallic lead was introduced into a long appendix attached to the discharge tube.

[a] e-mail: fizjk@univ.gda.pl

The lead was distilled under vacuum in several steps into last part of the appendix closest to the main discharge tube. Then the rest of the appendix was cut off under vacuum. The discharge tube and the metal container were surrounded by separate furnaces. Helium was used as buffer gas. The pressure of the buffer gas was about 5 Torr.

The discharge was excited by a rf oscillator (100 MHz) connected to the discharge tube by external electrodes. The optimum conditions for excitation i.e. the metal vapour and the buffer gas pressures and the oscillator power for each individual line were found separately.

The high resolution spectral apparatus consisted of a silver-coated Fabry-Perot etalon and Carl Zeiss Jena PGS-2 grating spectrograph (1200 grooves/mm, resolution 0.8 nm/mm in the first order) combined with a CCD detector (Hamamatsu model C7041 with head device model S7031-1006).

3 The computer program for IS analysis

It was assumed that the observed contour is described by the following intensity distribution function:

$$I(\tilde{\nu}) = C \sum_{i}^{N} \frac{I_0^i}{1 + \alpha_1^2 (RL + \delta\tilde{\nu}_i)^2 + \alpha_2^4 (RL + \delta\tilde{\nu}_i)^4}, \quad (1)$$

where C is the scaling factor, α_1, α_2 are the line shape parameters, N is the number of isotopes and hfs components, I_0^i is the maximum intensity of the ith component (proportional to the transition probability and percentage admixture of each isotope), RL is the adjustable parameter in the wave number scale, and:

$$\delta\tilde{\nu}_i = \delta\tilde{\nu}_i^{up} - \delta\tilde{\nu}_i^{down}. \quad (2)$$

In equation (2) $\delta\tilde{\nu}_i^{up}$ and $\delta\tilde{\nu}_i^{down}$ are the wave number shifts of the energy levels in respect to the position of the centre-of-gravity for the upper and lower multiplets respectively.

The first step in the computer analysis involves finding the positions and relative intensities of all the individual components. This procedure accepts the required atomic data of the investigated line, first of all the I and J quantum numbers of the two energy levels involved. The next procedure sorts all the components according to the wave number. Then the intensity distribution function (1) is employed to calculate the sum of intensities at each point of the final pattern using estimated values for the line profile coefficients.

In the next step the least-squares-fitting procedure is used; the simulated structure is compared with the experimental curve recorded in the digital form. The experimental profile is linearized and afterwards is normalized. Later the simulated contour is fitted to the experimental one by variation of suitable parameters. In this procedure the Marquardt's algorithm [5] is used.

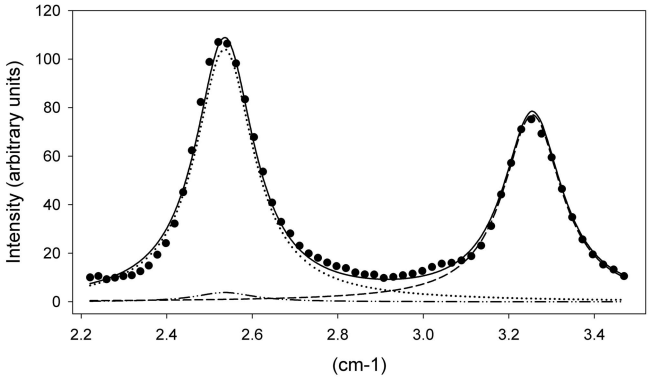

Fig. 1. The hfs of the 424.5 nm line. Black dots represent the experimental trace obtained with a 2 mm Fabry-Perot spacer. Here, the best fit was obtained for $A_{up} = 0.03$ mK and $A_{down} = 239.95$ mK (solid line). Dotted and dashed lines are contributions of different hfs components.

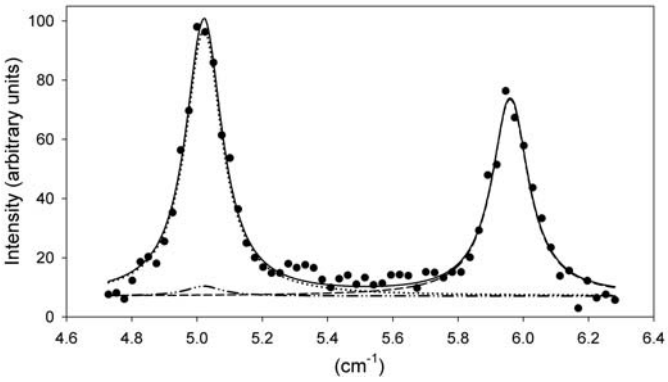

Fig. 2. The hfs of the 537.2 nm line. Black dots represent the experimental trace obtained with a 2 mm spacer. The best fit was obtained for $A_{up} = 0.01$ mK and $A_{down} = 316.03$ mK. Dotted and dashed lines are contributions of different hfs components.

4 Results and discussion

4.1 Hyperfine structure study

The hfs splittings of five lines of the Pb II were measured in metallic isotope ^{207}Pb. Figures 1–5 present the recorded hyperfine patterns of the observed lines. For studies of the 424.5 nm line we used 2 mm and 6 mm Fabry-Perot spacers. The recording time was about 60 min. For studies of the 537.2 nm line we used 2 mm and 4 mm spacers and the recording time was about 20 min. For studies of the 554.5 nm line 4 mm and 5 mm spacers were used. The recording time was about 60 min. Spectra of 560.9 nm and 666 nm lines were recorded in about 20 min; we used 7 mm and 8 mm spacers. For all the spectra we analyzed the first three visible interference orders.

The observed line contours were analyzed by the use of the least-squares-fitting procedure described in Section 3. In Figures 1–5 black dots represent experimental results and the solid line is the best fit described by

Table 1. Hfs constants for several levels of Pb II (in mK).

Configuration	Level	Line (nm)	$A^{\text{Present study}}$	$A^{\text{Other papers}}$
$6s^2 7d$	$^2\mathrm{D}_{5/2}$	554.5	73.32 (0.93)	73.7 (5.0)[a]
$6s^2 5f$	$^2\mathrm{F}_{7/2}$	537.2	0.04 (0.08)	
		424.5	0.50 (0.39)	
			0.06 (0.08)*	0[a]
$6s^2 7p$	$^2\mathrm{P}_{3/2}$	560.9	12.82 (0.87)	
		554.5	12.18 (1.33)	
			12.62 (0.73)*	∼20.0 (5.0)[a]
	$^2\mathrm{P}_{1/2}$	666.0	70.63 (0.49)	∼80.0 (5.0)[a]
$6s^2 6d$	$^2\mathrm{D}_{5/2}$	424.5	240.63 (0.95)	238.0 (5.0)[a]
				243.0 (1.0)[b]
$6s^2 7s$	$^2\mathrm{S}_{1/2}$	560.9	353.46 (1.94)	
		666.0	350.93 (2.04)	
			352.26 (1.41)*	350.0 (5.0)[a]
				348.0 (1.0)[b]
$6s6p^2$	$^4\mathrm{P}_{5/2}$	537.2	317.84(1.61)	319.0 (5.0)[a]
				310.0 (2.0)[b]

*Weighted mean value. [a]Reference [6]; [b]reference [7].

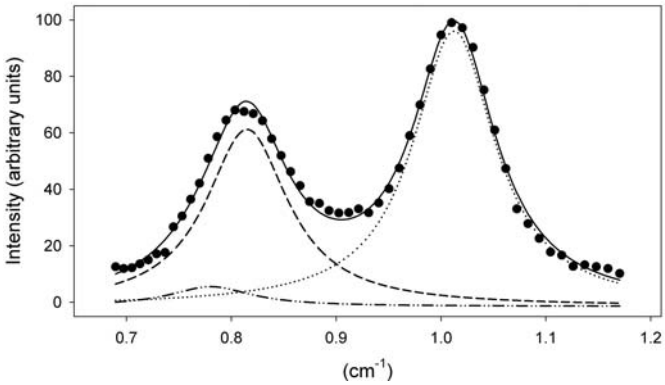

Fig. 3. The hfs of the 554.5 nm line. Black dots represent the experimental trace obtained with an 5 mm spacer. For the example presented here the best fit was obtained for A_{up} = 73.35 mK and A_{down} = 12.19 mK. Dotted and dashed lines are contributions of different hfs components.

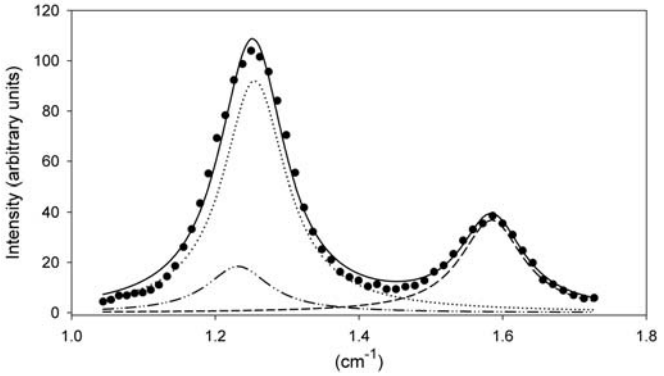

Fig. 4. The hfs of the 560.9 nm line obtained with 8 mm spacer. The best fit was obtained for A_{up} = 11.71 mK and A_{down} = 343.89 mK. Dotted and dashed lines are contributions of different hfs components.

formula (1). The dashed and dotted lines represent contributions to the total intensity from each hfs component. The computer simulations yielded the A hyperfine constants presented in Table 1 for following levels: $6s^2 7d\ ^2\mathrm{D}_{5/2}$, $6s^2 5f\ ^2\mathrm{F}_{7/2}$, $6s^2 7p\ ^2\mathrm{P}_{3/2}$, $^2\mathrm{P}_{1/2}$, $6s^2 6d\ ^2\mathrm{D}_{5/2}$, $6s^2 7s\ ^2\mathrm{S}_{1/2}$ and $6s6p^2\ ^4\mathrm{P}_{5/2}$.

Each value given in the table represents the average of several measurements performed under different experimental conditions. The numbers in brackets are the standard deviations. In some cases the A constants were calculated as a weighted means of values obtained from the observation of two different atomic lines.

In Table 1 also experimental results of other authors [6,7], obtained by the use of various experimental techniques, are given for comparison. Our results are in good overall agreement with earlier studies. An exception is the value for the $6s^2 7p\ ^2\mathrm{P}_{3/2}$ level — our result is about 37% lower than that one obtained by Rose [6].

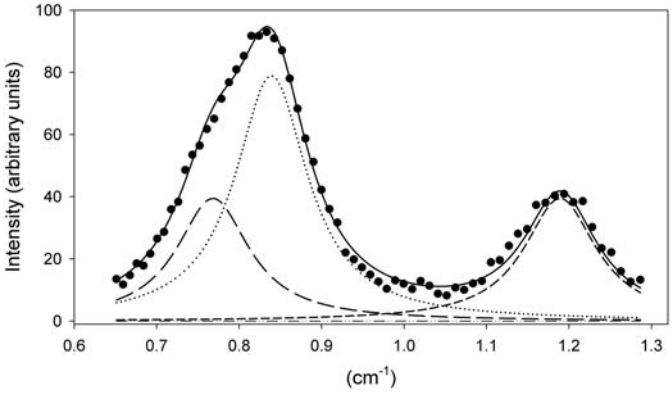

Fig. 5. The hfs of the 666 nm line. Here, the experimental trace was obtained with 7 mm spacer. The best fit was obtained for A_{up} = 70.92 mK and A_{down} = 350.31 mK. Dotted and dashed lines are contributions of different hfs components.

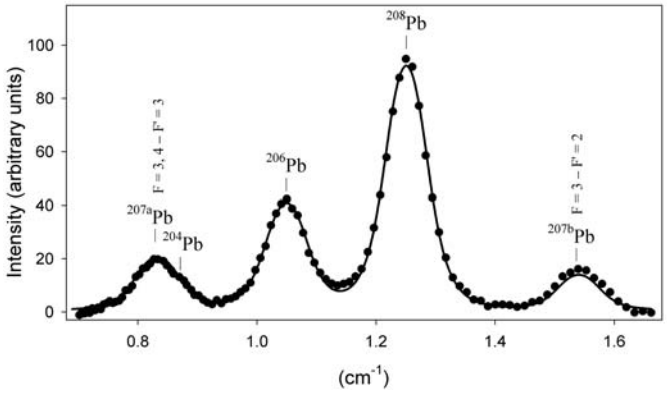

Fig. 6. The profile of the 424.5 nm line of natural lead. Black dots represent the experimental trace obtained with a 4 mm Fabry-Perot spacer and the solid line is the calculated best fit. The net line profile follows exactly the partial contributions from different isotopes — the isotope structure is well separated.

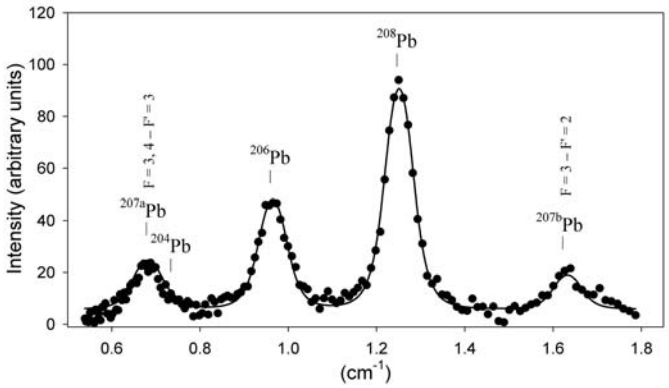

Fig. 7. The profile of the 537.2 nm line of natural lead. Black dots represent the experimental trace obtained with a 4 mm Fabry-Perot spacer and the solid line is the calculated best fit. The net line profile follows exactly the partial contributions from different isotopes — the isotope structure is well separated.

Results from Table 1 were used in further studies of isotope shifts in lines of natural lead.

4.2 Isotope shift study

Figures 6–10 present the recorded experimental results and calculated best-fit curves for the investigated lines of natural lead. In these studies Fabry-Perot spacers and recording times were the same as in hfs measurements.

The observed line contours were analyzed by the use of last-squares-fitting procedure described in Section 3. In Figures 6–10 black dots represent experimental results and the solid lines are the best fits described by formula (1). In the fitting procedure, the hyperfine splitting constants from Table 1 and theoretical relative intensity ratios of

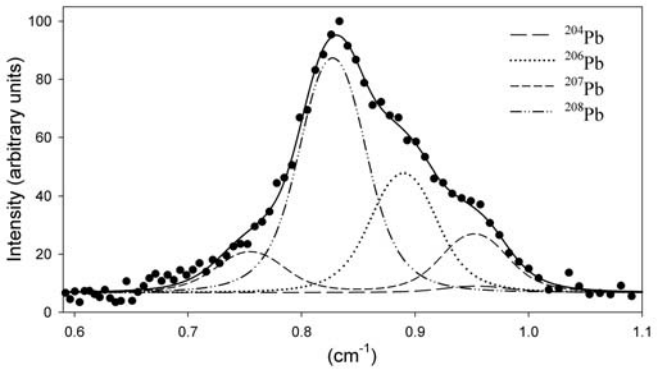

Fig. 8. Spectrum of the 554.5 nm line with appeared isotope shifts. Black dots represent the experimental trace obtained with a 6 mm Fabry-Perot spacer and the solid line is the best fit.

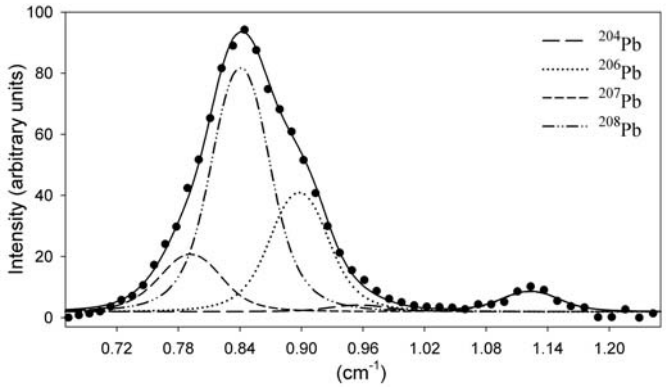

Fig. 9. Spectrum of the 560.9 nm line with appeared isotope shifts. Black dots represent the experimental trace obtained with a 6 mm Fabry-Perot spacer and the solid line is the best fit.

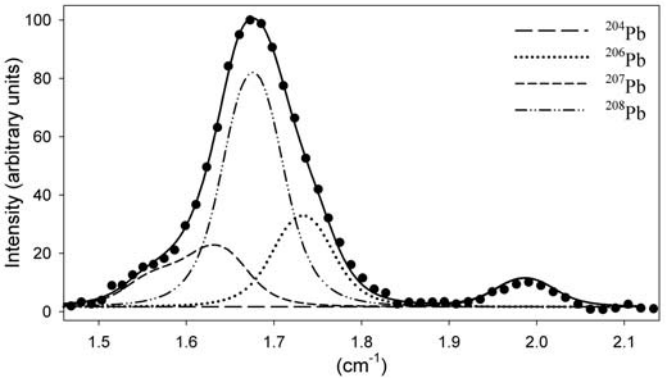

Fig. 10. Spectrum of the 666.0 nm line with appeared isotope shifts. Black dots represent the experimental trace obtained with a 6 mm Fabry-Perot spacer and the solid line is the best fit.

Table 2. Measured isotope shifts relative to ^{208}Pb (in mK).

Line No.	Line (nm)	$\delta\nu_i^{208-207_{CG}}$	$\delta\nu_i^{208-206}$	$\delta\nu_i^{208-204}$
1	424.5	127.40 (1.45)	202.38 (0.78)	387.00 (5.00)
2	537.2	175.98 (1.69)	283.13 (2.43)	535.00 (5.00)
3	554.5	–41.00 (0.98)	–65.15 (0.91)	–123.00 (5.00)
4	560.9	–36.85 (0.63)	–58.60 (0.54)	–112.00 (5.00)
5	666.0	–35.21 (0.61)	–56.52 (0.57)	–109.00 (5.00)

Numbers in brackets are standard deviations.

Table 3. Percentage abundance of lead isotopes of masses 204, 206, 207, 208.

	204	206	207	208
Reference [8]	1.5	23.6	22.6	52.3
Reference [9]	1.04	27.03	17.65	54.28
Present work	1.48 (0.16)	25.02 (2.24)	15.31 (1.80)	58.18 (2.07)

Numbers in brackets are standard deviations.

hfs components were used as fixed parameters. For all the spectra we analyzed the first three visible interference orders. The dashed and dotted lines represent contributions of each isotope to the total intensity.

The computer simulations yielded the isotope shifts presented in Table 2. Each value represents the average of several measurements performed under different experimental conditions. The numbers in brackets are standard deviations.

Table 3 presents the isotopic composition of the lead sample used in our experiment in comparison to average admixtures of isotopes occurring in natural lead. Derived by us admixtures were obtained as maxima of peaks of the line profile function (1).

The observed isotope shift $\delta\nu_i^{A'A}$ between two isotopes with mass numbers A' and A ($A' > A$) in an atomic spectral line i of frequency ν_i consists of two effects: a mass shift $\delta\nu_{i,MS}^{A'A}$ and a field (or volume) shift $\delta\nu_{i,FS}^{A'A}$ (see [10,11]):

$$\delta\nu_i^{A'A} = \delta\nu_{i,MS}^{A'A} + \delta\nu_{i,FS}^{A'A}. \tag{3}$$

The mass shift $\delta\nu_{i,MS}^{A'A}$ can be expressed as:

$$\delta\nu_{i,MS}^{A'A} = M_i\frac{A'-A}{A'A}. \tag{4}$$

It is a sum of two contributions: normal mass shift $\delta\nu_{i,NMS}^{A'A}$ and specific mass shift $\delta\nu_{i,SMS}^{A'A}$:

$$\delta\nu_{i,MS}^{A'A} = \delta\nu_{i,NMS}^{A'A} + \delta\nu_{i,SMS}^{A'A}. \tag{5}$$

These shifts depend, in the same way, on atomic masses A' and A:

$$\delta\nu_{i,NMS}^{A'A} = N_i\frac{A'-A}{A'A}, \tag{6}$$

$$\delta\nu_{i,SMS}^{A'A} = S_i\frac{A'-A}{A'A}. \tag{7}$$

Then, the mass shift factor $M_i = N_i + S_i$. The specific mass shift describes the phenomena of correlations between electrons, so the specific mass shift factor S_i is very difficult to calculate. As a matter of fact, good theoretical calculations of S_i exist for only a few elements and in all other cases rather rough estimates have to be used. In contrast to S_i, the normal mass shift factor N_i can easily be calculated as:

$$N_i = \frac{m_e}{m_n}\nu_i = \frac{\nu_i}{1822.9}. \tag{8}$$

For complex atoms in addition to the effect of finite mass there is the effect of finite size of the nucleus. The field shift $\delta\nu_{i,FS}^{A'A}$ can be expressed as:

$$\delta\nu_{i,FS}^{A'A} = F_i\lambda^{A'A}, \tag{9}$$

where F_i is an electronic factor and $\lambda^{A'A}$ is a nuclear parameter, which can be expressed as a power series of mean nuclear charge radii differences:

$$\begin{aligned}\lambda^{A'A} &= \delta\langle r^2\rangle^{A'A} + \frac{C_2}{C_1}\delta\langle r^4\rangle^{A'A} + \frac{C_3}{C_1}\delta\langle r^6\rangle^{A'A} + ... \\ &\cong K\delta\langle r^2\rangle^{A'A},\end{aligned} \tag{10}$$

where at C_i are the Seltzer coefficients [12]. For light elements the K factor is very close to 1 and decreases with increasing Z number. For lead $K = 0.93$ and was determined with an accuracy of 2% [13,14].

4.3 King plots

Equation (3) can be rewritten as:

$$\mu^{A'A}\delta\nu_i^{A'A} = M_i\frac{A'_{std}-A_{std}}{A'_{std}A_{std}} + F_i\mu^{A'A}\lambda^{A'A}, \tag{11}$$

where for arbitrarily chosen pair of standard isotopes A'_{std} and A_{std}:

$$\mu^{A'A} = \frac{A'A}{A'-A}\frac{A'_{std}-A_{std}}{A'_{std}A_{std}}. \tag{12}$$

Then a plot, for each observed optical transition i, of modified isotope shift $\mu^{A'A}\delta\nu_i^{A'A}$ versus modified nuclear parameter $\mu^{A'A}\lambda^{A'A}$ for different isotope pairs yields a straight line of intercept $\delta\nu_{i,MS}^{A'_{std}A_{std}}$ and slope F_i. This so called King plot contains as many points as there are isotope pairs. The multiplication of equation (3) by the factor containing A_{std} in expression (11) facilitates the reading of the King plot; the intersection of the regression line with y-axis gives directly the value of the mass shift [10,11,15].

Table 4. Values of the nuclear parameters $\lambda^{A'A}$ used in the King plot analysis (in fm^2).

Isotopic pair	$\lambda^{A'A}$	Reference	$\lambda^{A'A}_{\text{combined}}$
208–207	0.0540 (0.0418)	Electron scattering [11]	0.0737 (0.0052)
	0.0625 (0.0102)	Muonic X-ray [16]	
	0.0720 (0.0130)	K_α X-ray [17]	
	0.0800 (0.0070)	K_α X-ray [18]	
208–206	0.0978 (0.0418)	Electron scattering [11]	0.1184 (0.0053)
	0.1304 (0.0215)	Muonic X-ray [16]	
	0.0990 (0.0150)	K_α X-ray [17]	
	0.1210 (0.0060)	K_α X-ray [18]	
208–204	0.2392 (0.0412)	Electron scattering [11]	0.2231 (0.0075)
	0.2454 (0.0184)	Muonic X-ray [16]	
	0.2050 (0.0220)	K_α X-ray [17]	
	0.2200 (0.0090)	K_α X-ray [18]	

Numbers in brackets represent accuracy of the experimental data.

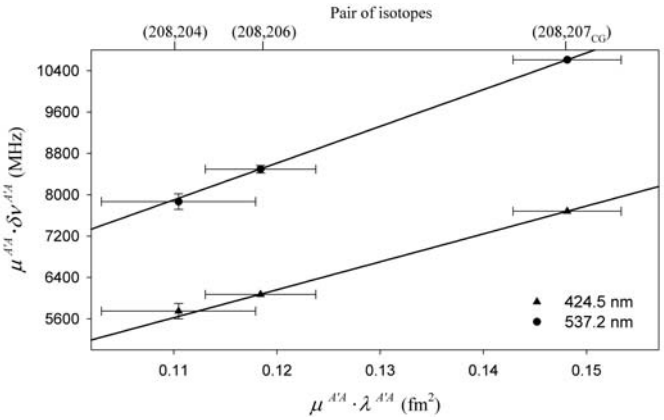

Fig. 11. King plots for 424.5 nm and 537.2 nm lines. The solid lines are linear regression lines — standard deviations of measuring points were used as weights in the fitting procedure.

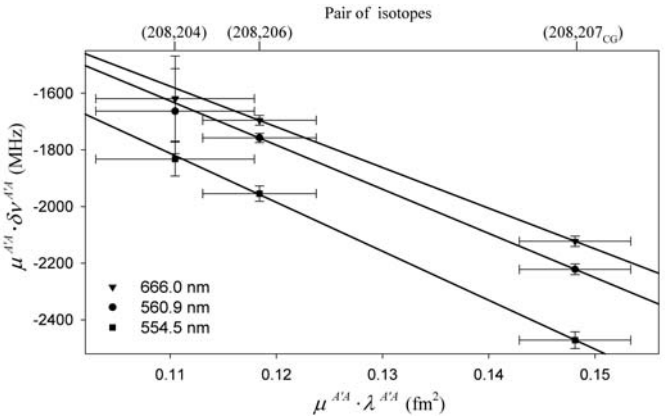

Fig. 12. King plots for 554.5 nm, 560.9 nm and 666.0 nm lines. The solid lines are linear regression lines — standard deviations of measuring points were used as weights in the fitting procedure.

Table 5. Results of the King plot analysis: electronic factors F_i and mass shift factors M_i (normal N_i and specific S_i).

λ (nm)	F_i (GHz/fm^2)	M_i (GHz)	N_i (GHz)	S_i (GHz)
424.5	53.97 (14.35)	–6772 (1090)	388	–7159 (1090)
537.2	71.68 (5.20)	–147 (220)	306	–423 (220)
554.5	–17.28 (1.41)	1881 (120)	297	1579 (120)
560.9	–15.58 (3.42)	1858 (455)	293	1565 (455)
666.0	–14.35 (4.30)	59 (564)	247	–188 (564)

Numbers in brackets are standard deviations.

We have performed this analysis with independent set of data on $\lambda^{A'A}$ presented in Table 4. In calculations we used combined results for $\lambda^{A'A}$ obtained as weighted mean values of results from electron scattering experiment [11], muonic X-ray [16] and K_α X-ray [17,18] data. The King plots for investigated atomic lines are presented in Figures 11 and 12.

The derived values of F_i and M_i are presented in Table 5. After the values of F_i and M_i have been determined the measured frequency shifts can be used for calibration values of $\lambda^{A'A}$ for the isotope chain. Results of this calculations are presented in Table 6; obtained by us values are compared with theoretical results [11] and experimental values from laser spectroscopic studies of isotope shifts in the 283.3 nm resonance line of Pb I [11].

4.4 Relative isotope shift and odd-even staggering

The fact that both the mass and the field effects factorize into a nuclear part and electronic one leads to interesting properties which can be described by the relative isotope shift (RIS). In this paper the relative isotope shift was expressed as the $\nu_{207_{CG}} - \nu_{206}$ shift normalized to the $\nu_{208} - \nu_{206}$ one. It is obvious that, if one of the isotope effects, either the mass or the field effect, is equal zero, the RIS should have the same value for all lines. Moreover, the relative isotope shift is approximately independent of the particular transition in which the shifts are measured, thus the RIS permits to compare the results from different atomic transitions.

Obtained by us experimental RIS values for studied transitions are listed in Table 7. At the bottom of the table experimental results of other authors [7,14] are given for comparison. As it can be seen the RIS values obtained in the present work are in satisfactory agreement (within ±1.5% range) with other experimental data.

Table 6. Derived values of the nuclear parameter and the changes of the mean square nuclear charge radii, in comparison with calculated and experimental results for the 283.3 nm line (in fm^2).

Isotopic pair	$\lambda^{A'A}$	$\delta\langle r^2\rangle^{A'A}$	$^{\dagger}\lambda^{A'A}_{\rm theory}$	$^{\dagger}\lambda^{A'A}_{283.3\ \rm nm}$
208–207	0.0733 (0.0018)	0.0789 (0.0020)	0.0712	0.0744 (0.0121)
208–206	0.1178 (0.0027)	0.1267 (0.0029)	0.1125	0.1194 (0.0195)
208–204	0.2210 (0.0045)	0.2377 (0.0049)	0.2248	0.2232 (0.0363)

†Reference [11].

Table 7. Relative isotope shifts in lead.

λ (nm)	$\frac{\nu_{207_{CG}}-\nu_{206}}{\nu_{208}-\nu_{206}}$	Reference
424.5	0.370 (0.003)	Present work
537.2	0.378 (0.004)	Present work
554.5	0.371 (0.006)	Present work
560.9	0.371 (0.005)	Present work
666.0	0.377 (0.005)	Present work
UV lines	0.376 (0.006)	[7]
283.3	0.375	[14]

In heavy atoms such as lead, isotope shifts are due, almost completely, to the field effect [7,10], so no differences between the RIS measured in different lines of the element are expected. However, such differences exist and can be interpreted in terms of non vanishing mass shift contribution [15]. Thus $\delta\nu_{MS} \neq 0$ values obtained from King's plot have independent confirmation in observed small changes of RIS values presented in Table 7.

It is interesting that all RIS values demonstrate the odd-even staggering effect, where the odd isotope center of gravity of the atomic line lies in longer distance to the heavier even isotope peak of the line profile. Let us define the staggering parameter γ, for an odd isotope A, as follows (see [13,14]):

$$\gamma = \frac{2(\langle r^2\rangle^A - \langle r^2\rangle^{A-1})}{\langle r^2\rangle^{A+1} - \langle r^2\rangle^{A-1}} = \frac{2(\delta\nu^{A'A} - \delta\nu^{A'A-1} - M_i/[A(A-1)])}{\delta\nu^{A'A+1} - \delta\nu^{A'A-1} - 2M_i/[(A+1)(A-1)]}. \quad (13)$$

This parameter can be understood as a measure of the polarization of the proton core of the nucleus by the added (odd) neutron relative to the effect of adding a neutron pair. Therefore γ equals one if there is no staggering and zero if the odd isotope has a charge radius equal to that of the next lowest isotope. The right side of equation (13) shows that γ can be deduced without a knowledge of the F_i – factors, but with reasonable estimate of M_i.

The average value of the staggering parameter for ^{207}Pb II was found to be $\gamma = 0.747(0.008)$. Our value is fully consistent with those given by other authors. For comparison, the γ value obtained from observation of several UV lines of ^{207}Pb II was found to be 0.752 [7] and from measurement of isotope shifts of the 283.3 nm resonance line of ^{207}Pb I the γ parameter was determined as equal 0.750(0.004) [13,14].

References

1. T.J. Wąsowicz, R. Drozdowski, J. Kwela, Phys. Scripta **71**, 274 (2005)
2. T.J. Wąsowicz, R. Drozdowski, J. Kwela, Phys. Scripta (2005, in print)
3. R. Drozdowski, J. Heldt, Phys. Scripta **47**, 175 (1993)
4. D. Grabowski, R. Drozdowski, J. Kwela, J. Heldt, Z. Phys. D **38**, 289 (1994)
5. D.W. Marquardt, J. Soc. Indust. Appl. Math. **11**, 431 (1963)
6. J.L. Rose, Phys. Rev. **47**, 122 (1935)
7. S. Bouazza, Y. Guern, J. Bauche, J. Phys. B: At. Mol. Phys. **19**, 1881 (1986)
8. *Handbook of Chemistry and Physics*, edited by R.C. Weast, S.M. Selby, 46th edn. (Chemical Rubber Company, Cleveland, Ohio, 1965)
9. C.B. Collins, R.M. Farquhar, R.D. Russell, Phys. Rev. **88**, 1275 (1952)
10. W.H. King, *Isotope shifts in atomic spectra* (Plenum Press, New York, 1984)
11. G. Fricke, C. Bernhardt, K. Heilig, L.A. Schaller, L. Schellenberg, E.B. Shera, C.W. De Jager, At. Data Nucl. Data Tables **60**, 177 (1995)
12. E.C. Seltzer, Phys. Rev. **188**, 1916 (1969)
13. R.C. Thompson, M. Anselment, K. Bekk, S. Göring, A. Hanser, G. Meisel, H. Rebel, G. Schatz, B.A. Brown, J. Phys. G: Nucl. Phys. **9**, 443 (1983)
14. M. Anselment, W. Faubel, S. Göring, A. Hanser, G. Meisel, H. Rebel, G. Schatz, Nucl. Phys. A **451**, 471 (1986)
15. J. Bauche, R.-J. Champeau, Adv. At. Molec. Phys. **12**, 39 (1976)
16. D. Kessler, H. Mes, A.C. Thompson, H.L. Anderson, M. S. Dixit, C.K. Hargrove, R.J. McKee, Phys. Rev. C **11**, 1719 (1975)
17. P.L. Lee, F. Boehm, Phys. Rev. C **8**, 819 (1973)
18. G.L. Borchert, O.W.B. Schult, J. Speth, P.G. Hansen, B. Jonson, H.L. Ravn, J.B. McGrory, Nuovo Cim. A **73**, 273 (1983)